Study of the Magnetic Horn for Neutrinos from Stored Muons (nuSTORM)

Chu Hon Kin

Department of Physics, The Chinese University of Hong Kong
CERN Summer Student Programme
Supervised by Prof. Kenneth Long, Tiago Alves and Marvin Pfaff

25 August 2022

Abstract

In this article, the performance of the proposed magnetic horn to be used in the Neutrinos from Stored Muons, nuSTORM, facility is investigated. The meson production process is monitored using simulations. The target and horn geometry were created using pyg4ometry. A magnetic field region inversely proportional to the radius is defined in the horn. Using a FLUKA simulation, a 100 GeV proton beam impinges on the target inside the horn which then focuses and delivers the produced pions into the pion transfer line. Different horn currents were applied for the delivery of 2.64, 5 and 7.2 GeV/c pions. The phases spaces of the pion beam were plotted using ROOT. Setting the emittance to 0.2 cm, the Twiss parameters are determined to be $\alpha = -0.42 \pm 0.01$, $\beta = 410 \pm 1$ cm and $\gamma = 0.00287 \pm 0.00002$ cm^{-1} such that the best acceptance can be achieved.

I. Introduction

nuSTORM

The Neutrinos from Stored Muons facility, nuSTORM, is designed to produce neutrino beams with precisely known flavour composition and energy spectrum. The facility aims to deliver a definitive neutrino-nucleus scattering programme for measuring the neutrino interaction cross sections. Neutrinos are produced from decay of muons stored in a decay ring. The created beam consists of equal fluxes of electron- and muon-neutrinos related by initial polarity and the energy distribution can be determined using the storage ring instrumentation.

The design of the accelerator facility is illustrated in Figure 1 acquired from nuSTORM [1]. A proton beam strikes an Inconel target inside a magnetic horn. The produced pions are focused by the magnetic field of the horn, directed by a pion transfer line to the storage ring with an allowance of 10% momentum spread and decay to muons in the production straight of the ring. The ring is capable of storing muons with momentum from 1 GeV/c to 6 GeV/c and a momentum acceptance of ±16% to allow further decay. A detector is set beyond the production straight to detect neutrinos from pion flashes and muon decays.

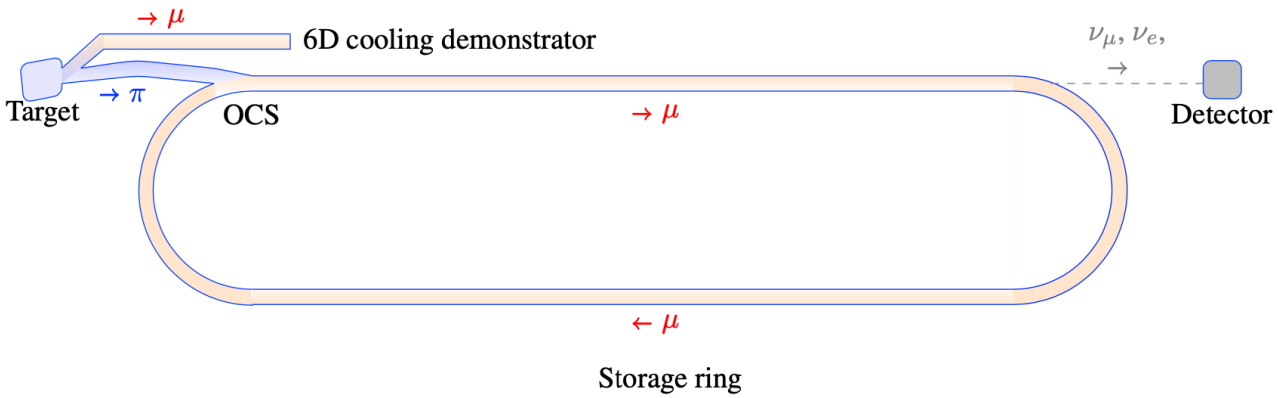

Figure 1: Schematic of the nuSTORM muon and neutrino beam facility. After a proton beam strikes the target, the produced pions are collected using a magnetic horn and directed into the transfer line which then transports pions to the nuSTORM storage ring. If the proton beam is extracted from CERN Super Proton Synchrotron, SPS, the produced pions can also serve a 6D muon ionisation cooling demonstration experiment. Figure from reference [1].

Currently, nuSTORM is in the stage of R&D to deliver a concrete proposal for implementing the infrastructure. The nuSTORM facility serves several purposes for high energy physics research. The well-defined flavour composition and energy spectrum of the neutrino beam allows for dedicated neutrino-nucleus scattering cross-sections measurements. Furthermore, the facility is capable of searching for physics beyond the Standard Model, for instance, the search for light sterile neutrinos [2]. The facility could also serve as a technological test bed for the development of a Muon Collider (6D Muon Cooling capabilities) or a Neutrino Factory.

Magnetic horn

A magnetic horn or neutrino horn is a device invented by Simon van der Meer at CERN for the focusing of neutrino beam. The horn has a magnetic channel that selects pions produced in the bombardment of the target and focuses them into a sharp beam.

In this article, we work on a horn designed for nuSTORM. The objectives are to simulate the pion production process, select pions within the momentum range and obtain the beam properties. As the horn locates at the beginning of the accelerator facility, the accepted pions set the initial conditions of the beam. The position-momentum distribution is important for quantifying the beam quality and matching the horn with appropriate optics. Knowledge from measurements of pion distribution parameters is required for accelerator design and phase space manipulation.

In addition, with the proposed implementation of nuSTORM at the SPS [3] which provides proton source beam at 100 GeV, the pions produced from the horn are suited for serving other experiments, including the 6D muon ionisation cooling experiment and ENUBET (Enhanced NeUtrino BEams from kaon Tagging; NP06).

II. Theory

A magnetic horn consists of an outer conductor and a coaxial inner conductor. When a current flows through the conductors in opposite directions, a magnetic field inversely proportional to the distance from the axis is created between the 2 surfaces of the conductors while no field exists inside the hollow tunnel of the inner conductor. The magnetic field region is filled with argon gas to limit the presence of nitrogen oxides and ozone so as to reduce corrosion and activation.

A target is placed inside the empty tunnel of the horn. When a beam coming from upstream bombards on the target, particles are produced and go in various directions. The magnetic field acts as a lens, bending particle trajectories. Particles that travel along the beamline will go downstream and leave the horn without experiencing any effect from the field while those that enter the field region will either be bent back to the centre or kicked out of the horn, depending on their charges. To avoid interactions with the particles passing through, the thickness of the inner conductor is set to be slim but able to withstand the magnetic force. Figure 2 is a horn prototype proposed by van der Meer [4] and the drawing demonstrates the general idea.

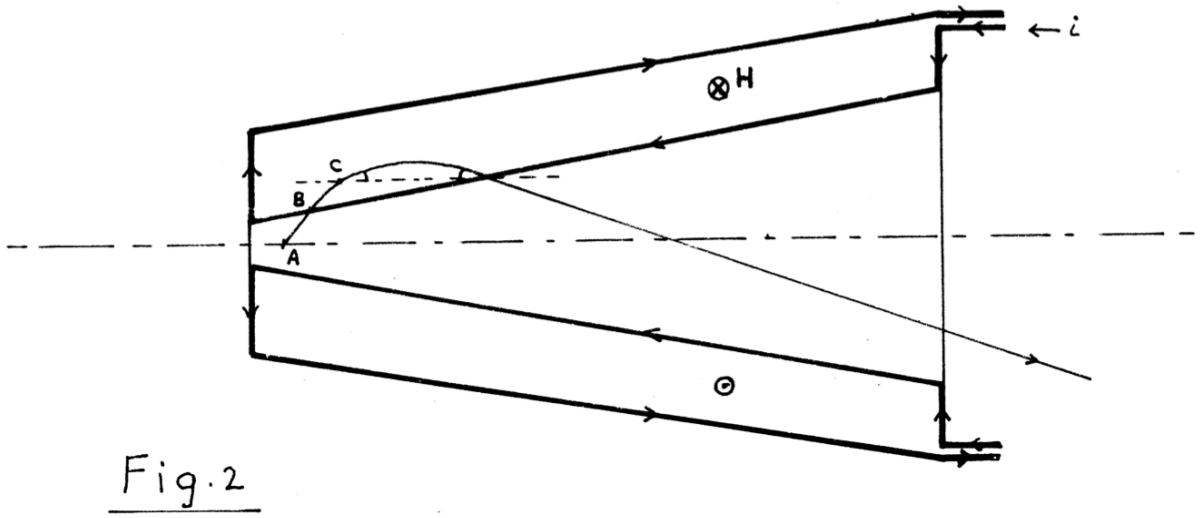

Figure 2: Van der Meer's original sketch of a magnetic horn. A negative particle is bent by the magnetic field, returns to the hollow centre and becomes less deviated. Figure from reference [4].

The direction of the horn current circulating inside the inner and outer conductor, referred to as current polarity, determines what pion charge is favoured. A current flowing antiparallel to the beam in the outer conductor produces a magnetic field that focuses positive pions and vice versa. Therefore the polarity of the current can be defined accordingly.

The pion transfer line is designed to deliver pions with a $\pm 10\%$ spread of momentum p_π. Pions within the momentum range are prioritized by the horn using the magnetic field. The magnetic field strength is directly proportional to the horn current. As a result, optimisation study is required to understand the relation of horn current and pion momentum.

III. Methods

The meson production process and the behaviour of pions leaving the horn are simulated using codes from nuSTORM. The workflow is to first build the geometry and set the parameters. Then the magnetic field is defined according to the horn current. Finally, pion production is simulated by running the beam bombardment on the target.

The geometry of horn and target is defined using pyg4ometry. The horn is made of a 2.2 m long aluminium cylinder, with a 10 cm outer conductor radius and a 2 cm inner conductor radius. The upstream (downstream) is created by digging from the edge of the front (back) end to 25 cm (1.1m) inside the horn and the radius decreases from 8.5 cm (5.0 cm) to the length of inner conductor radius. Also the interior of the aluminium conductor is carved out and filled with argon gas, leaving the conductor to be 2.5 mm thick. More specifications regarding the curvatures of the upstream and downstream can be found in the Appendix. The target is a 46 cm long cylinder with a radius of 6.3 mm. It is placed inside the hollow tunnel of the horn right after the upstream. The target is made of Inconel, other materials, such as graphite, can also be considered. The dimensions of the horn are visualised in Figure 3. The geometry can be used in either FLUKA or BDSIM.

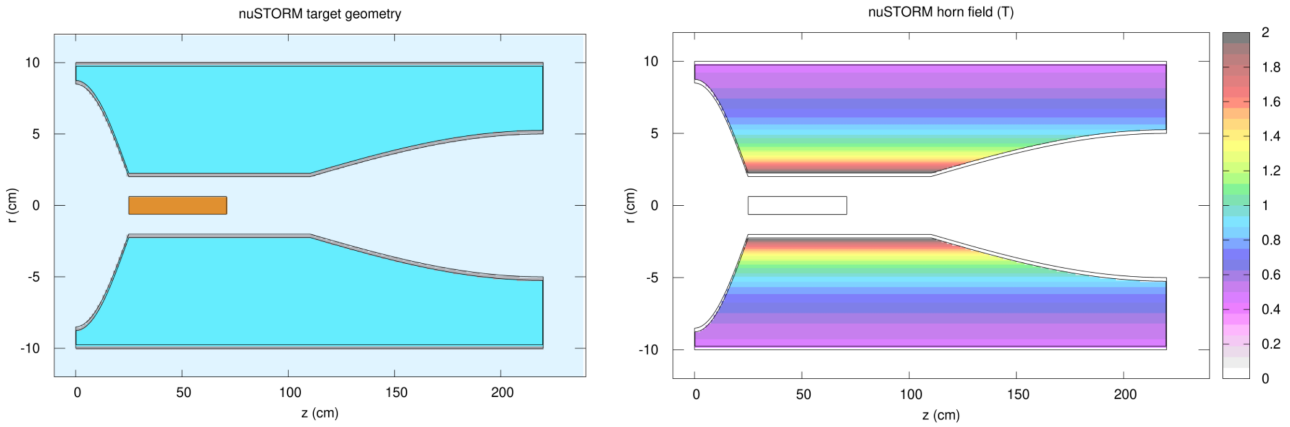

Figure 3: Left: The horn and target geometry. The aluminium conductor is labelled in grey, the argon gas region in blue and the target in orange. Right: The magnetic field gradient inside the horn. The magnetic field only exists in the argon gas region. The longitudinal axis is labelled in z direction. The upstream edge is set at z = 0. Note that the conductor is 2.5 mm thick along the edges of both ends.

The pyg4ometry file also define the beam and current parameters. To imitate the implementation of nuSTORM at the SPS, the beam energy is set at 100 GeV. A gaussian distribution beam model is applied with 2.67 mm standard deviation. From Fermilab optimisation study [5], the horn current is set at 219 kA for 5 GeV/c pions. The horn current I is estimated to be linearly proportional to the pion momentum p_π, that is

$$I = \frac{219}{5}\, p_\pi \tag{1}$$

The 315.4 and 115.6 kA current are applied for selecting 7.2 and 2.64 GeV/c pion. The 0 kA current option is used for simulating the no horn situation. The horn polarity is set to be +1 and −1 for selecting positive and negative pion respectively.

The magnetic field is only defined in the argon gas region. With the argon gas position and the horn current I, the field strength B is given by

$$B = \frac{\mu_o I}{2\pi r} \tag{2}$$

where r is the radial distance. Together with the current polarity pol, the field vector can be specified in cartesian coordinates:

$$\mathbf{B} = [-pol\ B\ sin(\phi),\ pol\ B\ sin(\phi),\ 0] \tag{3}$$

where ϕ is the azimuthal angle. The gradient of the magnetic field strength is shown in Figure 3 as well.

With the defined geometry, beam parameters and magnetic field, the beam bombardment on the target can be simulated using FLUKA. Although different kinds of particles are produced at the target, only the kinematics of pions and muons are tracked. Much less kaons are produced and the number of neutrinos coming from kaon decays is below 1% cutoff for modelling, thus the contributions of kaon are neglected. Also, the beam will be further purified along the transfer line before entering the decay ring.

The output files contain distributions of Particle Data Group ID, total energy (in GeV), position (in cm), momentum (in GeV/c) and the likelihood weighting. Eight sample files are produced, four for each current polarity. Samples for 115.6, 219 or 315.4 kA currents contains 10 million proton-on target (POT) events and the aperture with 10 cm radius is located at the end of the downstream. Samples for 0kA contain 1 million POT events and record particles leaving the target surface from all directions.

IV. Results and Discussion

The samples produced from FLUKA simulations can be examined using ROOT Data Analysis Framework. The data analysis serves as a sanity check for the simulations and enables us to obtain the optical requirements for accepting the pion beam. In the following, only the results of the negative currents are shown, please refer to the Appendix for the positive currents.

The position coordinates of particles are plotted in Figure 4. Pions are selected by filtering the particles' PDGIDs. Without the presence of a horn current, the particles form a cylindrical surface. This confirms that the corresponding sample files contains all particles coming out from the target. Furthermore, most of the pions leaves at the curved surface of the target, thus the majority of the pions will be lost without the magnetic horn. Particles create a circular plate when there exists a horn current. This is because the corresponding files only record particles coming out from the output plane. Tiny amount of particles are seen behind the plate because the aperture is set to be 2 mm thick.

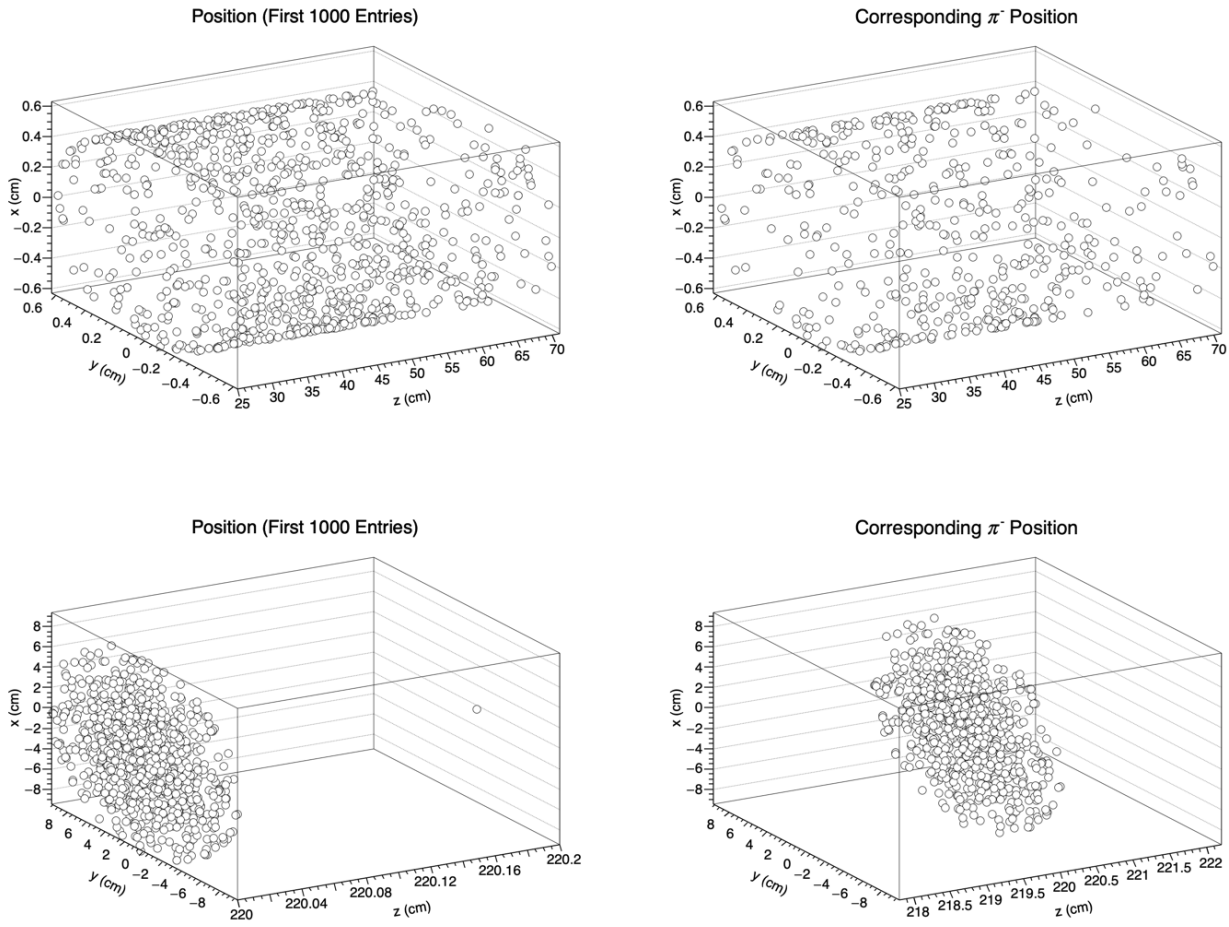

Figure 4: The longitudinal axis is set in z direction. Left: Particle positions. Only the first 1000 entries are shown for concise visualization. Right: Positions of the pions from the first 1000 entries. Top: The distribution on top is derived from the 0 kA simulation. The particles form the cylindrical surface of the target which is 46cm long. Bottom: The distribution at the bottom is derived from the -219 kA simulation. The particles are located at z = 220 cm which is the output plane right after the downstream of the horn. The tracking aperture is 2 mm thick and one entry is detected from behind.

The PDGID for each particle give the composition for each sample as shown in Table 1. The samples contain pions and muons as only these particles are tracked in the simulation. The files for no horn current only contain one tenth as much POT events for other files, the number of entries should be much higher otherwise. There are more entries in a file for higher current because more particles can be focused to the output of the horn. The ratio of π^+ to π^- produced is closed to unity as shown in the row for no current. However, negatively charged particles are favoured by the magnetic field created by a negative current and vice versa. This conforms to the working principle of the magnetic horn.

Table 1: Particle compositions for non-positive current samples

Current (kA)	Entries	π^-	π^+	μ^-	μ^+
-315	29419298	86.10%	10.46%	3.36%	0.08%
-219	23651640	82.86%	13.98%	3.06%	0.11%
-115	16465278	74.43%	23.00%	2.39%	0.19%
0	17137843	49.71%	50.10%	0.06%	0.13%

The pion energy distributions for different horn currents are shown in Figure 5. Only pions with charges that tally with the current polarity are selected by identifying their PDGIDs. The weight for each entry from no current sample is set to be 10 such that the POT is consistent with that of other samples (10^7 POT). For pions collected in the output plane, the distributions peak at 0.5 GeV. The peak position does not change with respect to the current due to the fact that the magnetic field does not do work on the particles.

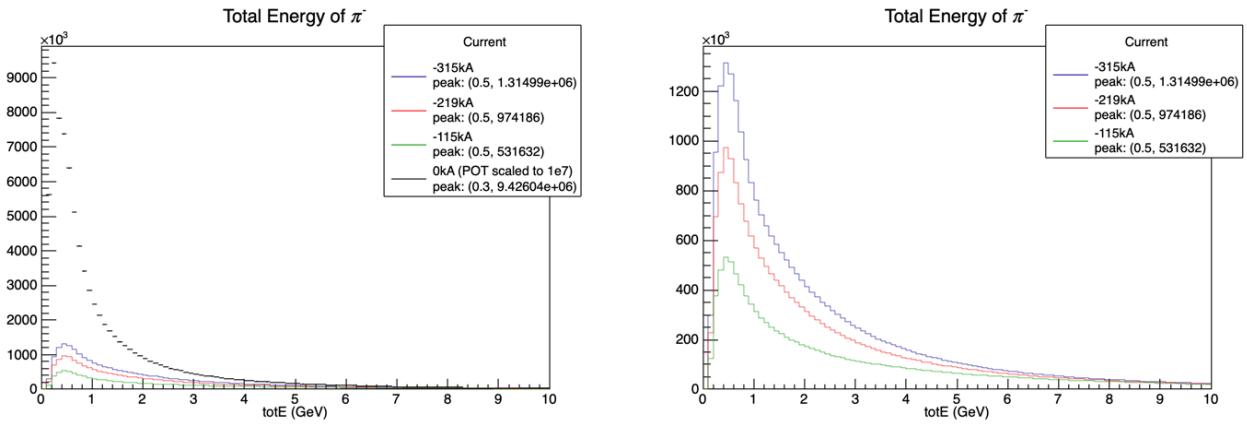

Figure 5: Left: The energy distributions of negative pion from non-positive current samples. The data from 0 kA sample are weighted by 10 such that the distribution corresponds to a scaled POT consistent with other samples. The 0 kA distribution is much higher than others because pions are tracked from every angle. Right: The energy distributions of negative pion from negative current samples. This clearer visualization shows that the peaks all locate at 0.5 GeV.

The transverse position in Figure 6 shows how the particle are distributed when they leave the output plane. As the transfer line accepts pions with an allowance of 10% momentum spread, not all pions that leave the horn are of interest. Therefore a cut flow is implemented on the pions according to their total momenta. For -219 kA current simulation, negative pions with momenta ranging from 4.5 GeV to 5.5 GeV constitute 3.9% of pions passing through the output plane. The distribution have the shape of a donut because the magnetic field directs particles to the centre. As the radius of the field-free region is 5cm in the downstream edge, this describes the outer radius of the donut.

A position-momentum phase space tells how the particles spread out along a certain direction. The particle momentum is a dimensionless parameter defined to be the momentum along the axis over the longitudinal momentum. The pion beam phase spaces for the transverse directions are shown in Figure 7. Only pions with the correct charges and momenta are included.

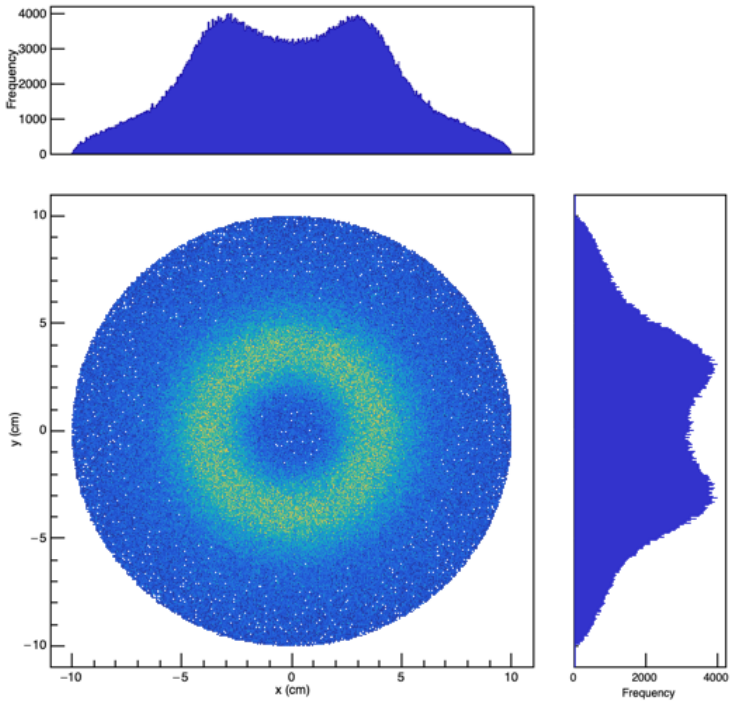

Figure 6: The transverse positions of 5 GeV/c negative pions from −219 kA simulation. The distribution appears to be a donut. The transverse axes are labelled in x and y directions. The projections on both directions are included.

The pion phase distribution can be broken down into the diagonal line, the dispersed region and the background. The diagonal line is independent of the magnetic field because pions in this line are those that never enter the magnetic field region. While pions from the dispersed region correspond to the pions that are focused and bent back by the magnetic field. Therefore the compactness of the dispersed region is subjected to the field strength. As shown in Figure 7, the phase distributions share similar shapes regardless of horn current. This indicates that the linear scaling of the current is a fair estimation for optimising pions with different momentum spreads. The background are deviated pions that are unlikely to be collected. With a stronger magnetic field and therefore stronger focusing power, the contributions from the background become smaller.

Knowing how the pions are distributed in the phase space, the pion acceptance can be maximized by determining the beam emittance and the Courant-Snyder parameters, also called Twiss parameters. The emittance ε measures the average spread of the coordinates on the phase space. It relates to the Twiss parameters α, β and γ by

$$\varepsilon = \gamma x^2 + 2\alpha x x' + \beta x'^2 \tag{4}$$

The equation traces an ellipse in the phase space. The emittance sets the area A of the ellipse by

$$A = \pi\varepsilon \tag{5}$$

α rotates the ellipse about the origin, β describes the extent the ellipse stretches out along the major axis and γ is defined by

$$\gamma = \frac{1+\alpha^2}{\beta} \tag{6}$$

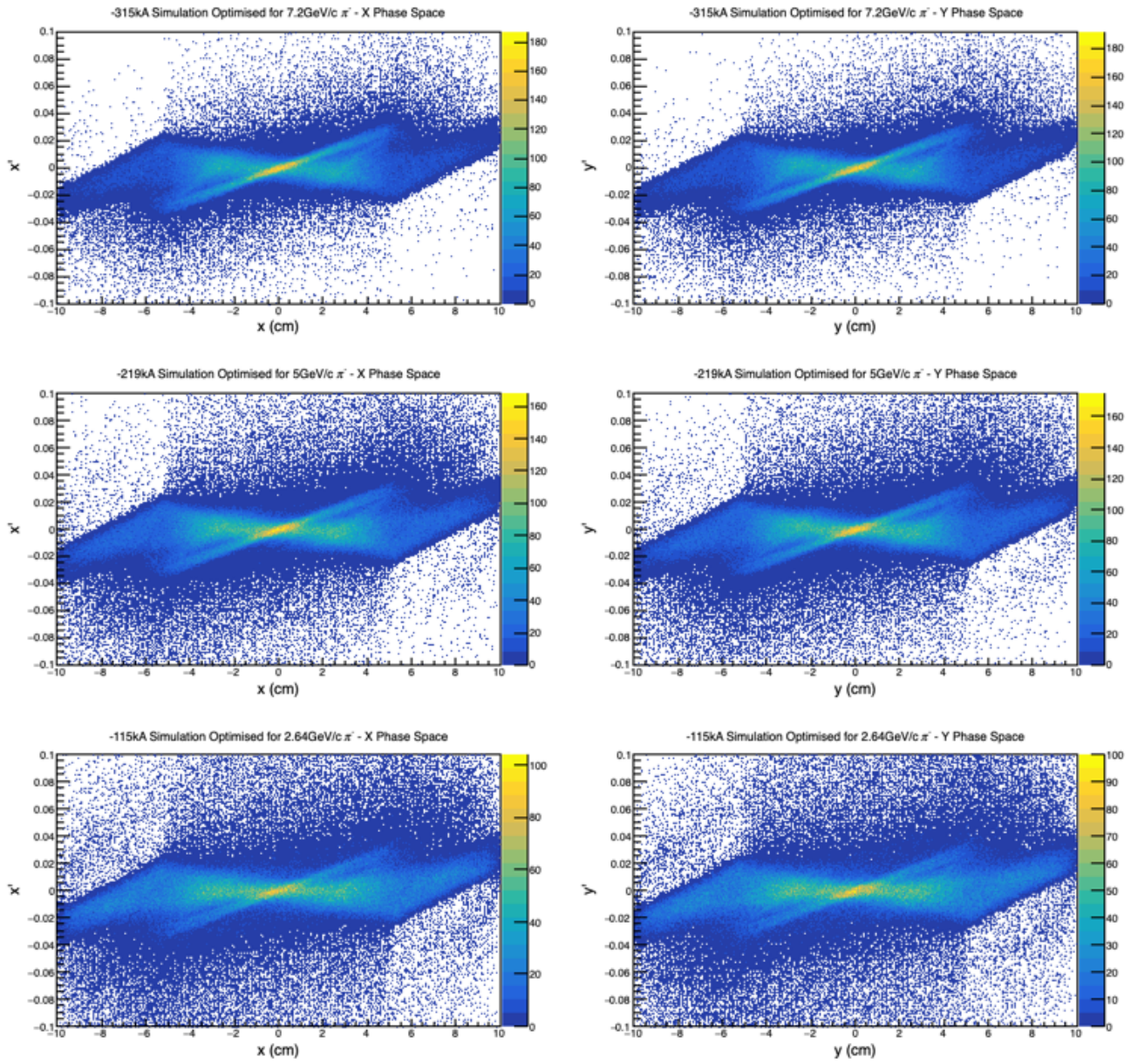

Figure 7: Phase spaces for different horn current simulations and directions. The position is plotted against the momentum along the transverse axes labelled in x and y directions. Left: x/x' phase spaces. Right: y/y' phase spaces. From top to bottom, the phase spaces contains π^- with 7.2, 5 and 2.64 GeV/c momenta and $\pm 10\%$ momentum spreads which originate from simulations of -315 kA, -219 kA and -115 kA currents respectively. The diagonal lines and the dispersed regions are confined similarly in different phase spaces. The backgrounds are more significant in phases spaces for pions with lower momenta.

The acceptance is the region that the ellipse encloses in the phase space, particles that fall within the ellipses in both x- and y-phase space will be accepted by the transport line.

As the emittance affects the aperture of the magnets in the transfer line, it is set in place to be 0.2 cm. Then the values of α and β are tuned to form the best phase space acceptance for incoming pions. As the shapes of the phase spaces in Figure 7 are consistent, the calculated parameters are applicable to different horn currents and transverse directions. Here, the pion acceptance is optimised for -219 kA simulation. The Twiss parameters are worked out to be $\alpha = -0.42 \pm 0.01$, $\beta = 410 \pm 1$ cm and $\gamma = 0.00287 \pm 0.00002$ cm^{-1}. Figure 8 shows the ellipse plotted in the phase spaces. The pion acceptance for each simulation is listed in Table 2.

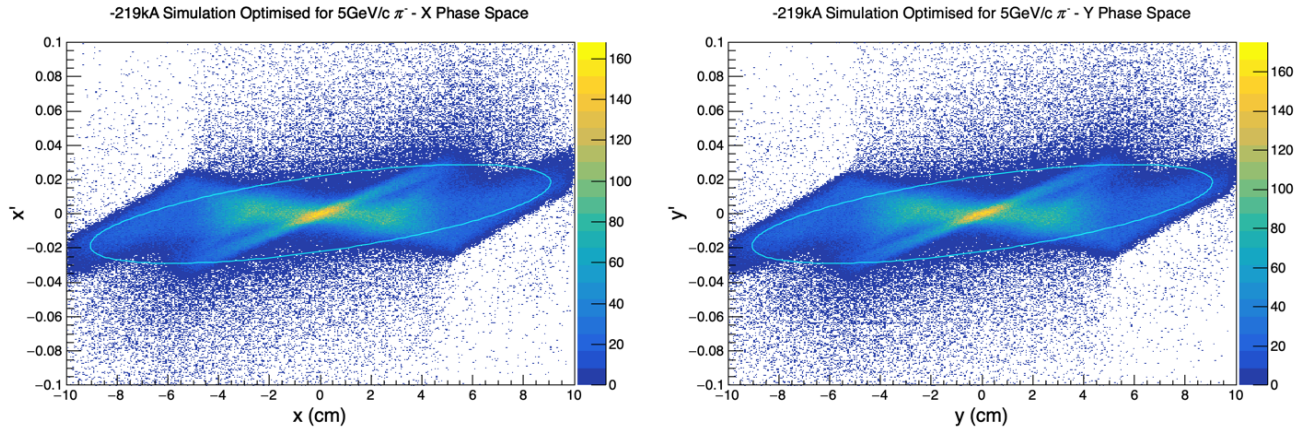

Figure 8: The acceptance ellipse plotted in phase space. Pions enclosed by the ellipses in both dimensions are accepted. α and β are optimized to provide the best pion acceptance. The equation of the ellipse is $0.02 = 0.00287x^2 - 0.84xx' + 410x'^2$ (applied equivalently to y and y').

Table 2: Pion acceptance with respect to the charge and momentum

	2.64 ± 10% Gev/c	5 ± 10% Gev/c	7.2 ± 10% Gev/c
π^-	66.0%	75.6%	80.4%
π^+	66.3%	75.9%	80.5%

V. Summary

This study focuses on the magnetic horn and the produced pion beam from nuSTORM. The target and horn geometry in addition to the proton beam properties are defined in pyg4ometry. The horn current responsible for creating the magnetic field is optimised for 2.64, 5 and 7.2 GeV/c pions. The proton beam strikes on the target to produce pions in a FLUKA simulation. The phase spaces of the pion beam are analysed using ROOT. To have the best pion acceptance, the Twiss parameters are calculated to be $\alpha = -0.42 \pm 0.01$, $\beta = 410 \pm 1$ cm and $\gamma = 0.00287 \pm 0.00002$ cm^{-1} with the emittance being constrained to 0.2 cm.

Acknowledgements

I would like to express my sincere gratitude to Prof. Kenneth Long, Tiago Alves and Marvin Pfaff, who supervised and guided me through the project. I would also like to thank William Shields for giving a tutorial on BDSIM and John Back for providing clarification on the pyg4ometry file. It is a pleasure to participate in the summer programme organized by CERN Summer Student Programme Committee and the financial support from the Physics Department at the Chinese University of Hong Kong is greatly appreciated.

References

[1] L. A. Ruso, T. Alves, S. Boyd, A. Bross, P. R. Hobson, P. Kyberd, J. B. Lagrange, K. Long, X.-G. Lu, J. Pasternak, M. Pfaff, & C. Rogers (for the nuSTORM collaboration), *Neutrinos from Stored Muons (nuSTORM)*, arXiv:2203.07545.

[2] nuSTORM Collaboration, D. Adey *et al.*, *Light sterile neutrino sensitivity at the nuSTORM facility*, arXiv:1402.5250.

[3] C. C. Ahdida *et al.*, *nuSTORM at CERN: Feasibility Study*, CERN Document Server, CERN-PBC-REPORT-2019-003.

[4] S. van der Meer, *A directive device for charged particles and its use in an enhanced neutrino beam*, CERN Document Server, CERN-61-07.

[5] A. Liu, A. Bross, & D. Neuffer, *Optimization of the magnetic horn for the nuSTORM non-conventional neutrino beam using the genetic algorithm*, Nuclear Instruments and Methods in Physics Research Section A: Accelerators, Spectrometers, Detectors and Associated Equipment, Vol. 794, 11 Sep 2015, p. 200-205.

Appendix

A. Horn geometry

The curvatures of the horn upstream and downstream are described in cylindrical coordinates with z representing the longitudinal axis.

$$\begin{aligned} upstream : r &= r_f + (r_i - r_f)\ cos(\frac{\pi}{2}\frac{z - z_i}{z_f - z_i}) \\ downstream : r &= r_i + (r_f - r_i)\ sin(\frac{\pi}{2}\frac{z - z_i}{z_f - z_i}) \end{aligned} \quad , \ z \in [z_i, z_f] \tag{7}$$

The initial and final values of the coordinates are labelled with subscripts i and f respectively. The interior and exterior surfaces of each stream obey the same equation but with different initial and final values specified in Table 3.

Table 3: Initial and final values of (r, z)

Stream	Surface	z_i (cm)	z_f (cm)	r_i (cm)	r_f (cm)
upstream	exterior	0	25	8.5	2
upstream	interior	0.25	25	8.75	2.25
downstream	exterior	110	220	2	5
downstream	interior	110	219.75	2.25	5.25

B. Positive current samples

There are simulations of the horn with positive currents, namely 115.6, 219 and 315.4 kA, they are optimised for 2.64, 5 and 7.2 GeV/c π^+ respectively. The positive current samples are treated in the analogous manner as the negative ones.

Table 4: Particle compositions for non-negative current samples

Current (kA)	Entries	π^-	π^+	μ^-	μ^+
315	29880856	9.14%	87.48%	0.07%	3.31%
219	24031887	12.16%	84.75%	0.09%	3.00%
115	16707648	19.81%	77.68%	0.15%	2.36%
0	17132589	49.69%	50.11%	0.06%	0.13%

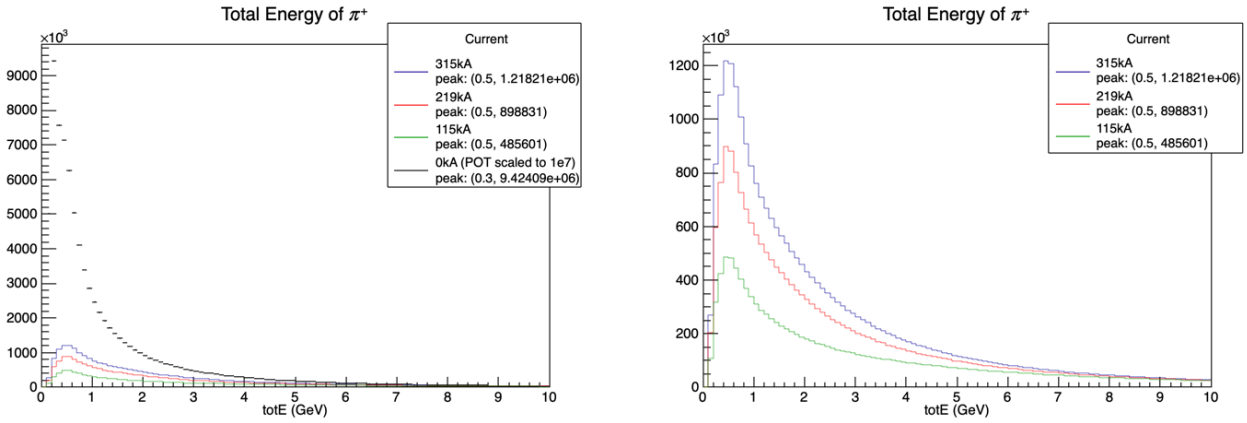

Figure 9: Left: The energy distributions of positive pion from non-negative current samples. Right: The energy distributions of positive pion from positive current samples.

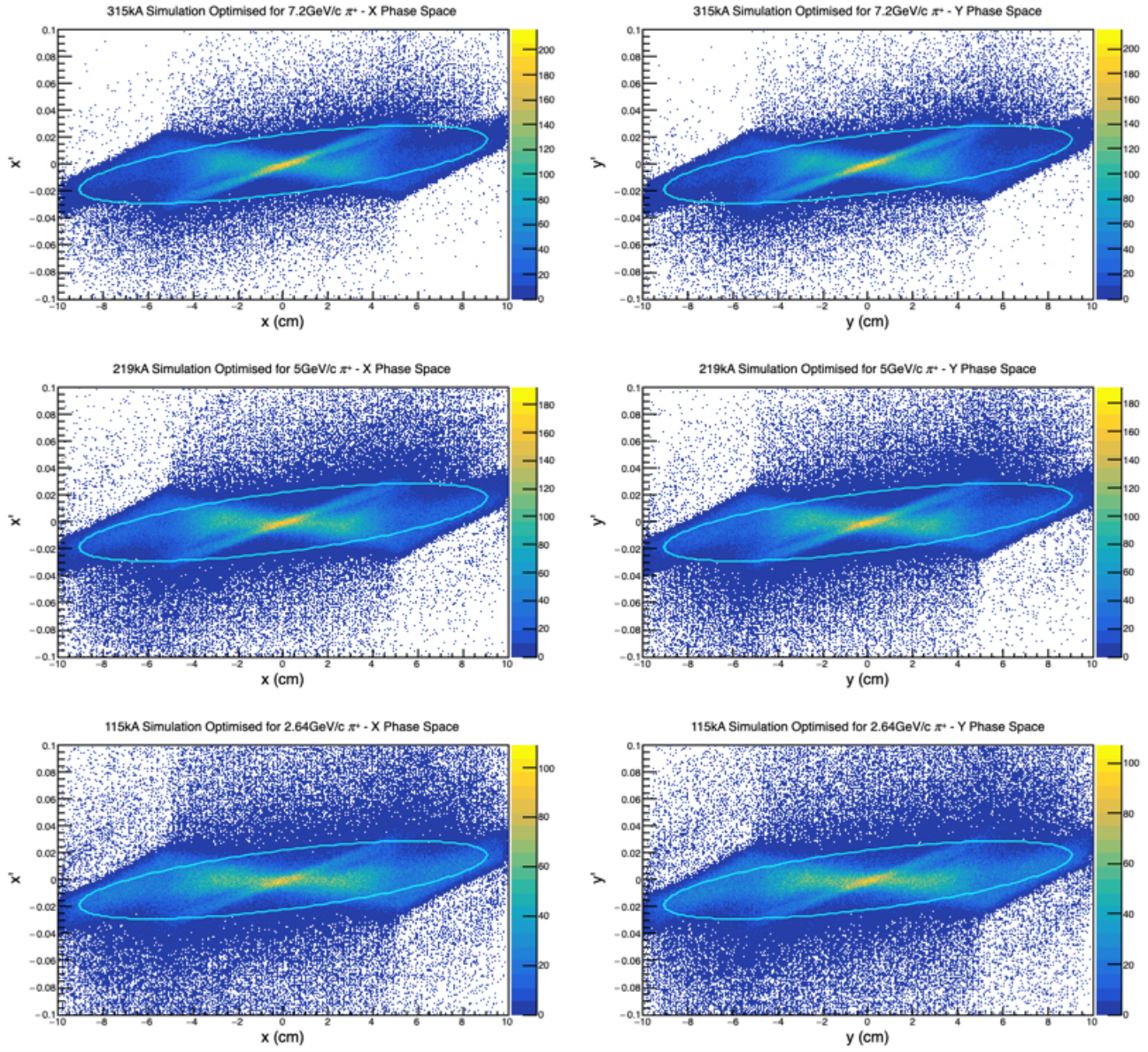

Figure 10: The acceptance ellipse plotted in π^+ phase spaces from positive horn current samples.